Biochemical and Biophysical Research Communications **270,** 67–75 (2000)
doi:10.1006/bbrc.2000.2377, available online at http://www.idealibrary.com on IDEAL®

Isolation of a Novel PDZ-Containing Myosin from Hematopoietic Supportive Bone Marrow Stromal Cell Lines

Tadashi Furusawa, Shuntaro Ikawa, Nobuaki Yanai, and Masuo Obinata
Department of Cell Biology, Institute of Development, Aging, and Cancer, Tohoku University, Seiryo-machi, Aoba-ku, Sendai 980-8575, Japan

Received February 22, 2000

Stromal cells in bone marrow provide an optimal microenvironment for hematopoiesis. The established stromal cell lines from bone marrow showed various cellular heterogeneities and differed in their hematopoietic supportive ability. By a differential display method, we cloned a gene whose expression levels were correlated with the hematopoietic supportive ability of stromal cells. Its deduced amino acid sequence shows a structure similar to myosins, except that it lacks an actin binding site. Interestingly, it contains a KE-rich sequence and a PDZ domain in the NH_2-terminal, which are protein–protein interaction domains; therefore we termed this novel myosin Myosin containing PDZ domain (MysPDZ). Western blot analysis showed that its protein levels positively correlated with the supportive ability of stromal cells and immunostaining suggested that MysPDZ was present at cytoskeleton in a filamentous and/or network form. Thus MysPDZ may be involved in the maintenance of the stromal cell architectures required for cell to cell contact.

Key Words: **myosin; PDZ domain; bone marrow stromal cells; hematopoietic supportive ability.**

The hematopoietic system is regulated by a microenvironment consisting of stromal cells in bone marrow (1–7). In addition to soluble factors and extracellular matrices, direct cell to cell communication between stromal cells and hematopoietic cells may be required for the regulation of proliferation and differentiation. Stromal cells in bone marrow show morphologically distinct subsets of cells, which may reflect their hematopoietic supportive abilities (8, 9).

We have isolated panels of stromal cell lines from temperature sensitive (ts) SV40 T-antigen transgenic mice (10) and demonstrated that these cell lines showed various hematopoietic supportive ability (10–12). In this work, using a differential display method, we isolated a gene whose expression level was correlated with the hematopoietic supportive ability of the stromal cells. The deduced amino acid sequence from the isolated full length cDNA shows a novel protein with similarity to myosins, and it has a KE (lysine and glutamine)-rich sequence followed by a PDZ domain in the NH_2-terminal, thus we call it MysPDZ.

MATERIALS AND METHODS

Cell cultures. Mouse bone marrow stromal cell lines (TBR series) were established from ts SV40 T-antigen transgenic mice and were maintained as described previously (10). NIH3T3 cells were cultured in Dulbecco's modified eagle's medium (GIBCOBRL, Grand Island, NY) supplemented with 10% fetal bovine serum (FBS).

Enrichment of hematopoietic stem cells. Bone marrow cells obtained from C57BL/6 mice were suspended in staining buffer [0.2% bovine serum albumin (BSA)–Dulbecco's phosphate-buffered saline (PBS, pH 7.0)] and incubated with fluorescein isothiocyanate (FITC)-conjugated anti-lineage markers (B220, CD3, Mac-1, Gr-1 and Ter119, Pharmingen, San Diego, CA), phycoerythrin (PE)-anti-Sca-1 (Pharmingen) and biotinylated anti-c-Kit (ACK2, kindly provided by Dr. S.-I. Nishikawa, Kyoto University, Japan) (13). They were then incubated with allophycocyanin (APC)-streptavidin (Becton Dickinson, San Jose, CA). After the final wash, cells were suspended in staining buffer and kept on ice prior to fluorescence-activated cell sorting (FACS).

Cobblestone colony assay. Stromal cells were cultured in 6-well plates (Falcon3046, Becton Dickinson) until sub-confluency at 33°C, then the temperature was shifted to 37°C and the medium was changed to α-minimum essential medium (α-MEM, Flow Laboratories, Irvine, CA) containing 10% FBS and 50 μM 2-mercaptoethanol (2-ME). Co-cultivation with hematopoietic cells was begun 3 days after the temperature shift. Lin^-/c-Kit^+/Sca-1^+ hematopoietic cells were sorted by FACStar^{PLUS} (Becton Dickinson) with 200 cells per well and the medium was changed every 3 days for 2 weeks. Foci containing more than 10 hematopoietic cells beneath the stromal cell layers were counted as cobblestones by inverted-phase microscopy. The supportive ability was shown as a percentage of total cobblestone colony number of TBR31-1 for 2 weeks culture.

Differential display. RNAs were prepared from stromal cells cultured under the identical condition of cobblestone colony assay. RNAs were treated with RNase-Free DNase (RQ-1, Promega, Madison, WI) and 2.5 μg of total RNAs were reverse transcribed for 1 h at 45°C in 10 μl of first strand synthesis reaction mix (5× first strand

0006-291X/00 $35.00

buffer, 10 mM ditiothreitol, 0.2 mM dNTP, 100 units of MMLV-reverse transcriptase, SuperScript II, GIBCOBRL) using 2.5 μM of 3 different oligo dT primers; T_{17}GX, (5′-TTTTTTTTTTTTTTTTGX-3′), T_{17}CX (5′-TTTTTTTTTTTTTTTTCX-3′), and T_{17}AX (5′-TTTTTTTTTTTTTTTTAX-3′). The reaction mixture was 25-fold diluted with Tris-EDTA buffer (10 mM Tris-HCl, 0.2 mM EDTA, pH 8.0) and 2.5 μl of the resultant mixture was added to an equal volume of polymerase chain reaction (PCR) reaction mix [1× PCR buffer, 1.5 mM $MgCl_2$, 2 μM dNTP, 0.025 μl of ^{32}P-dCTP (3000 Ci/mmol), 25 μM of both forward and reverse primers, 2.5 units of Taq DNA polymerase (GIBCOBRL), and 0.6 μg of Taq antibody (CLONTECH, Palo Alto, CA)]. PCR was performed with 12 different combinations of the last two 3′ bases anchored oligo $(dT)_{14}$ reverse primers and eight 13-mer arbitrary forward primers. PCR reaction was done with 25 or 30 cycles at 95°C for 30 s, 36°C for 30 s, 72°C for 30 s, then 10 min longer at 72°C. PCR products were applied on a 6% acrylamide gel in Tris-glycine buffer (250 mM Tris, 1.92 M glycine). The resultant gel was blotted on a piece of filter paper and then exposed on X-ray film. The bands of interest on a gel were located by oriented film and cut out. Gel slices were boiled in 100 μl of water at 95°C for 10 min, and 1.0 μl of supernatant of the extract was applied for reamplification by PCR using the same primers as the differential display.

Northern blotting. RNAs extracted from stromal cell lines and tissues were separated by 1% agarose gels and transferred to nylon membranes. Following prehybridization, blots were hybridized overnight in hybridization buffer with ^{32}P-labeled probe prepared from a cDNA fragment (nucleotide 2442–4842).

Cloning of full-length MysPDZ cDNA. The correlation of CB17-2, one of 91 cDNA fragments, was confirmed with supportive ability resulting from Northern blot analysis. Data base search found KIAA0216 (DDBJ/EMBL/GenBank accession number D86970), entried by Kazusa DNA Research Japan, which showed significant homology to CB17-2. To clone the full length cDNA of CB17-2, the ^{32}P-labeled probe was prepared from SmaI fragment (nucleotide 1483–4421, 2939 bp) of KIAA0216 cDNA kindly provided by Kazusa DNA Research Japan and 1,700,000 plaques of λ ZIP Lox C57BL/6 mouse spleen cDNA library were screened. To obtain the 5′ region, PCR was applied to a mouse spleen cDNA library using internal primer (5′-ACGGCGCATGCTCATCTCTTCCAGG-3′) and T7 (5′-TAATACGACTCACTATAGGG-3′) or SP6 (5′CATACGATTTAG-GTGACACTATAG-3′) primers located in λ ZIP Lox phage arms. Sequence of the 5′ region was determined by direct sequencing and the region was cloned by PCR.

Antiserum against MysPDZ. The cDNA fragment encoding the coiled-coil domain (residues 1732–1943, Fig. 3) was subcloned into pGEX 5X-1 vector (Amersham Pharmacia biotech). The glutathione S-transferase-MysPDZ fusion protein (GST-MysPDZ1732-1943) was purified by GST Purification Modules (Amersham Pharmacia biotech). GST-MysPDZ1732-1943 was treated with Factor Xa (New England Biolab) to cleavage at the fusion joint. Antisera against recombinant MysPDZ (rMysPDZ1732-1943) were raised by immunization of rabbits. Immunoglobulin G (IgG) fraction of antisera were purified by protein A Sepharose column (AmpurePA Kit, Amersham Pharmacia biotech), followed by affinity purification against the antigen coupled to a column (HiTrap NHS-activated, Amersham Pharmacia biotech).

Western blot analysis. Stromal cell cultures were rinsed with PBS and harvested by scraping in cold RIPA buffer (50 mM Tris-HCl, pH 8.0, 150 mM NaCl, 0.5% deoxycholate, 1% NP-40, 2 mM $MgCl_2$, 2 mM $CaCl_2$, 0.1% sodium azide) containing protease inhibitors [10 μg/ml soybean trypsin inhibitor, 1 U/ml aprotinin, 1 mM phenylmethylsulfonyl fluoride (PMSF), 1 μg/ml leupeptin]. Protein samples (20 μg/lane) were applied on SDS-polyacrylamide gel electrophoresis (SDS-PAGE). After electrophoresis, proteins were blotted onto nitrocellulose membranes. Filters were immunoblotted with anti-MysPDZ antibody diluted at 40 ng/ml, and bound antibodies were visualized by ECL Western blotting detection system (Amersham Pharmacia biotech).

cDNA transfection. Full length MysPDZ cDNA was subcloned into pCDNA3.1(−)/Myc-His expression vector (Invitrogen) in fusion with myc tag sequence at 3′-terminal. Expression vectors were transfected into NIH3T3 cells by calcium phosphate coprecipitation method and cells were fixed the next day for immunostaining.

Immunohistochemistry. Stromal cells and transfected NIH3T3 cells cultured on poly-L-lysine coated cover slips were incubated for 15 min at 37°C with microtubule stabilization buffer (100 mM PIPES, pH 7.0, 1 mM $MgCl_2$, 5 mM EGTA, 0.5 μM Taxol, 4% polyethleneglycol 4000, 0.5% Triton X-100) (14). Cells were fixed for 30 min at 4°C with 4% paraformaldehyde-PBS and incubated for 3 h at 4°C with staining buffer (2% BSA, 5% FBS-PBS). After blocking, cells were incubated with primary antibody diluted in staining buffer [for anti-MysPDZ antibody, 4 μg/ml; anti-β-tubulin (NEOMARKERS, Union City, CA), 1:50; anti-myc antibody, 1:1000]. After incubation, cells were washed with 0.1% Tween 20–PBS, and incubated with a second antibody. For staining by 3,3-diaminobenzidine tetrahydrochloride (DAB), biotinylated anti rabbit goat IgG (ZYMED) was used as the second antibody. After the incubation, cells were washed followed by incubation with HRP-conjugated avidin diluted at 1:500. After the final washing, cells were incubated with 0.05 M Tris-HCl, pH 7.6, 3 mg/ml DAB, 0.006% H_2O_2. For double labeling of MysPDZ and actin, cells were incubated in diluted FITC-labeled anti-mouse IgG (ZYMED) and 200 units/ml of rhodamine-labeled phalloidin (Molecular Probes, Eugene, OR). For double labeling of MysPDZ and β-tubulin, cells were incubated in diluted FITC-labeled anti rabbit antibody (Cappel, 1:500) and rhodamine-labeled anti mouse IgG.

Sequence analysis. Sequence similarity searches and motif searches were performed using FASTA, BLAST and MOTIF programs, run on a GenomeNet WWW server (http://www.genome.ad.jp/). The protein sequence alignments were produced with ClustalW (GenomeNet WWW server) and the philogenic tree was created by TreeView software (download from WWW site of Division of Environmental and Evolutionary Biology, Institute of the Biomedical and Life Sciences, University of Glasgow; http://taxonomy.zoology.gla.ac.uk/rod/rod.html). Prediction of the coiled-coil region was analyzed using MacStripe 2.0 software (15).

RESULTS

Cobblestone supportive ability among stromal cell lines. To measure the hematopoietic supportive ability of 20 stromal cell lines, Lin^-/c-Kit^+/Sca-1^+ hematopoietic cells were isolated by cell sorter and co-cultured with each cell line as previously reported. The supportive ability was expressed as the number of cobblestone colonies (Fig. 1). Twenty cell lines were classified into 3 groups: 5 cell lines with highly supportive (TBR59, 33, 357, 31-1 and 311), 11 poorly supportive (TBR52, 6, c, 10-1, 16-1, 91, 152, 17, 53, 9, and 511) and 4 with intermediate supportive ability (TBR11, 92, 343, and 351).

Differential display and isolation of a gene whose expression level is correlated with the supportive ability. We applied a differential display method to screen the genes whose expression levels were correlated with cobblestone supportive ability. Ninety-six different combinations of primer sets consisting of twelve anchored oligo(dT) primers and eight arbitrary primers were used. We isolated 91 differentially ex-

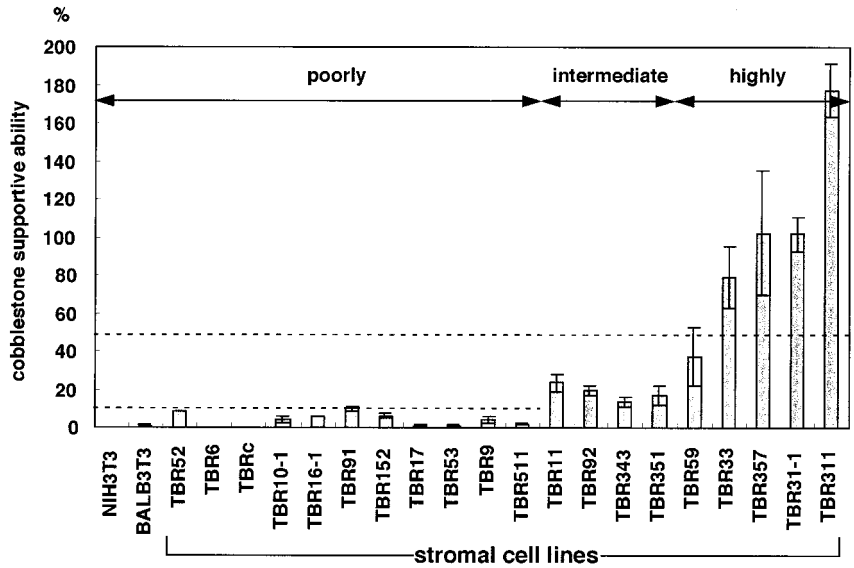

FIG. 1. Hematopoietic supportive ability among bone marrow stromal cell lines. Two hundred $Lin^{-}Sca\text{-}1^{+}c\text{-}Kit^{+}$ hematopoietic cells were co-cultivated with 20 stromal cell lines and the supportive ability was estimated by cobblestone colony formation. Data are means ± SD of 3 independent experiments. The supportive ability is shown as a percentage of cobblestone colony number of TBR31-1 after 2 weeks of culture. BALB3T3 and NIH3T3 mouse fibroblast cell lines were used as a control. The supportive ability was designated as poorly, intermediate, or highly.

pressed bands: 48 were chosen for their positive correlation with supportive ability and the others for their negative correlation. The average length of these bands was 220 bp. They were recovered from gels and reamplified using the corresponding primers. Using these cDNA fragments as probes, Northern blot analysis was performed to assess the results of differential display. The expression of one of these cDNA, CB17-2 was shown to correlate with supportive ability (Fig. 2). The sequence of this cDNA fragment was determined and a human homolog (KIAA0216) was found in DDBJ/EMBL/GenBank DNA databases (DDBJ/EMBL/GenBank Accession No. D86970) with an unknown function (16). We screened 1700,000 plaques of mouse spleen λ ZIP Lox cDNA library using human cDNA as a probe, and isolated 14 independent clones. The most extended cDNA clone, R2-2, contained a 7289 bp cDNA fragment, but the initiation codon was lacking in the 5′ region. To obtain the 5′ region, PCR was applied to the mouse spleen cDNA library using an internal primer of R2-2 and T7 or SP6 primers located in λ ZIP Lox phage arms. We found a termination codon upstream of the ATG provisional first codon at nucleotide position 52, and judged this ATG to be an initiation site. Its sequence is available from DDBJ/EMBL/GenBank DNA databases (DDBJ/EMBL/GenBank Accession No. AB026497).

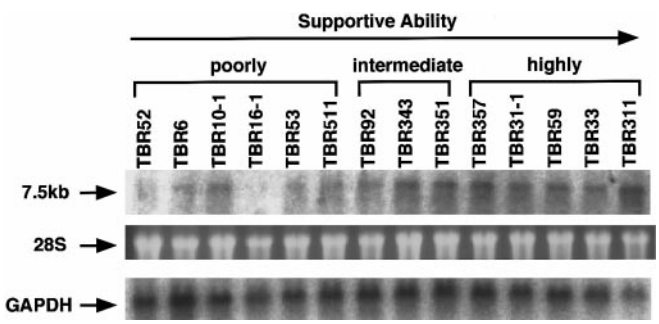

FIG. 2. MysPDZ mRNA expressions in stromal cell lines. Total RNA were prepared from each stromal cell and 10 μg RNA was applied on each lane. MysPDZ mRNA is observed as 7.5 kb transcript in the stromal cell lines. TBR52-92 have poorly hematopoietic supportive ability (poorly), TBR357-311 have highly supportive ability (highly), and TBR92-351 have intermediate supportive ability (intermediate). 28S indicates the amount of 28S ribosomal RNA and GAPDH indicates the expression level of glyceraldehyde-3-phosphate-dehydrogenase.

Sequence, motif and structure of MysPDZ. An open reading frame (ORF) of the CB17-2 gene encodes a protein of 2035 amino acid residues with unmodified relative molecular mass of 230 kDa. The amino acid sequence showed 94% homology with a human homolog (KIAA0216), but an additional 458 amino acids were present at the NH_2-terminal. BLAST programs revealed that the region of residues 407–2035 of this protein showed homology with myosins. Interestingly, a KE-rich sequence (residues 6–23) and a PDZ domain (residues 220–310) were found in the NH_2-terminal by SMART and ProfileScan programs, thus we called this molecule Myosin containing PDZ domain (MysPDZ). An unrooted phylogenic tree constructed from a region of the motor domains of 15 known myosin superfami-

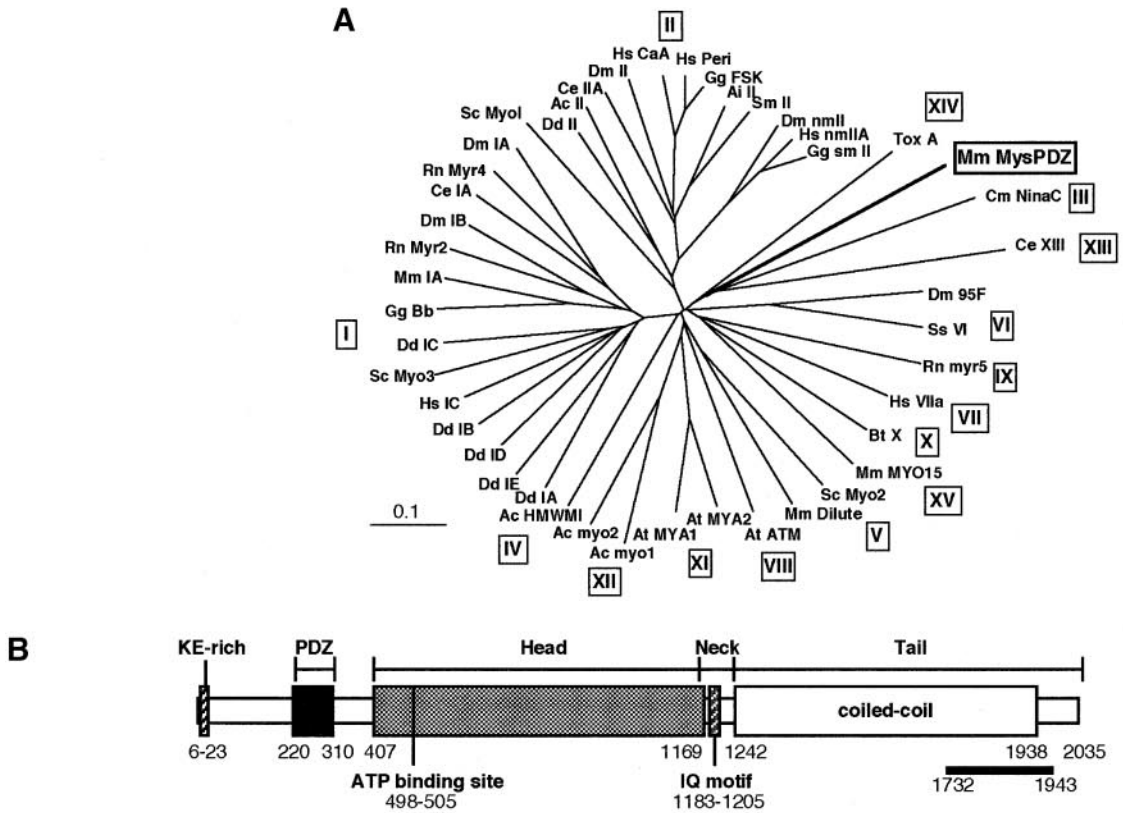
A
II
Hs CaA
Hs Peri
Dm II
Gg FSK
Ce IIA
Ai II
Ac II
Sm II
Sc MyoI
Dd II
Dm nmII
XIV
Dm IA
Hs nmIIA
Tox A
Gg sm II
Rn Myr4
Mm MysPDZ
Ce IA
Cm NinaC
III
Dm IB
Ce XIII
XIII
Rn Myr2
Mm IA
Dm 95F
Gg Bb
Ss VI
VI
I
Dd IC
Rn myr5
Sc Myo3
IX
Hs IC
Hs VIIa
Dd IB
VII
Bt X
Dd ID
X
Mm MYO15
Dd IE
Sc Myo2
Dd IA
XV
Ac HMWMI
Mm Dilute
0.1
At MYA2
Ac myo2
At MYA1
At ATM
V
IV
Ac myo1
XI
VIII
XII
B
KE-rich
PDZ
Head
Neck
Tail
coiled-coil
6-23
220 310 407
1169 1242
1938 2035
ATP binding site
498-505
IQ motif
1183-1205
1732 1943
C
Mm MysPDZ 6 KKDKDKDGGRKEKKEKKE 23
Hs MysPDZ 6 KKDKDKDGGRKEKKEKKE 23
Mm MAPB 640 KEIKTKLEEKKEEKPKKE 657
Hs IF-2 315 KKDKKKKGEKEEKEKEK 332
Sc NOP5 477 KKDKKEKKEKKEKKEKE 494
Sc CBF5 434 KKEKKEKKDKKEKKEKE 451
Dm T2FA 366 KKDKGKDEVSKDKKKKP 383
D
Mm MysPDZ 220 ELELQRRPTGDFGFSLRRTTMLDRAPEGQAYRRVVHFAEPGAGTKDLALG-LVPGDRLVEINGQNMENKSRDEIVEMIRQSGDSVRLKVQPI 310
Hs MysPDZ 220 ELELQRRPTGDFGFSLRRTTMLDRGPEGQACRRVVHFAEPGAGTKDLALG-LVPGDRLVEINGHNMESKSRDEIVEMIRQSGDSVRLKVQPI 310
Hs AF6 991 IITVTLKKQNGMGLSIVAAKGAGQ------DKLGIYVKSVVKGGAADVDGRLAAGDQLLSVDGRSLVGLSQERAAELMTRTSSVVTLEVAKQ 1076
Mm SAP-102 149 EIVLER-GNSGLGFSIAGGIDNPHV----PDDPGIFITKIIPGGAAAMDGRLGVNDCVLRVNEVDVSEVVHSRAVEALKEAGPVVRLVVRRR 235
Rn PSD-95 65 EITLER-GNSGLGFSIAGGTDNPHI----GDDPSIFITKIIPGGAAAQDGRLRVNDSILFVNEVDVREVTHSAAVEALKEAGSIVRLYVMRR 151
Dm DLG1 40 DIQLER-GNSGLGFSIAGGTDNPHI----GTDTSIYITKLISGGAAAADGRLSINDIIVSVNDVSVVDVPHASAVDALKKAGNVVKLHVKRK 126
Mm ZO1 23 TVTLHRAPGFGFGIAISGGRDNPHFQ---SGETSIYISDVLKGGPAEGQ--LQENDRVAMVNGVSMDNVEHAFAVQQLRKSGKNAKITIRRK 109
E
Mm MysPDZ 467 REDMAPHIYAVAQTAYRAMLMSRQDQSIVLLGSSGSGKTTSFQHLVQ 513
Hs MysPDZ 9 REDMAPHIYAVAQTAYRAMLMSRQDQSIILLGSSGSGKTTSCQHLVQ 55
Hs MYH3 148 RQEAPPHIFSISDNAYQFMLTDRENQSILITGESGAGKTVNTKRVIQ 194
Hs MYH8 150 RQEAPPHIFSISDNAYQFMLTDRENQSILITGESGAGKTVNTKRVIQ 196
Hs MYH11 32 RHEMPPHIYAIADTAYRSMLQDREDQSILCTGESGAGKTENTKKVIQ 78
Mm Dilute 132 MGDMDPHIFAVAEEAYKQMARDERNQSIIVSGESGAGKTVSAKYAMR 178
F
Mm MysPDZ 1185 SRHLTLFQAACRGYLARQHFK 1205
Hs MysPDZ 731 SRNLTLFQAACRGYLARQHFK 751
Hs MYH9 780 TDVIIGFQACCRGYLARKAFA 800
Hs MYH11 672 TDVIMAFQAMCRGYLARKAFA 692
Hs MYH10 787 TDIIIFFQAVCRGCLARKAFA 807
Hs IQGAP 746 EGLITRLQARCRGYLVRQEFR 766

lies with MysPDZ is shown in Fig. 3A. MysPDZ does not join any of the existing branches of the tree with greater than 60% confidence.

A schematic diagram of the domain structure of MysPDZ is shown in Fig. 3B. A KE-rich sequence is a nuclear targeting sequence conserved between nuclear proteins and centromere/microtubule binding proteins like TFIIF-α and MAP (Fig. 3C). Downstream of a KE-rich sequence, there is a PDZ domain, which is involved in protein-protein interaction. Alignment of the amino acid sequence of the PDZ domain of MysPDZ with that of other PDZ containing proteins is shown in Fig. 3D. We found that a genomic clone from human 17 chromosome (DDBJ/EMBL/GenBank Accession No. AC005412) contained an exon which showed significant similarity to nucleotide 1–946 of MysPDZ cDNA. It showed 88% homology at the nucleotide level and the deduced amino acid sequence (Hs MysPDZ in Fig. 3D) showed 94% homology. Nagase *et al.* (16) reported that KIAA0216 also located on chromosome 17, suggesting that MysPDZ has a specific variant in hematopoietic cells without a KE-rich sequence and a PDZ domain (see Northern blotting analysis).

Myosins share a common structural organization consisting of a conserved head domain followed by a myosin light chain/carmodulin binding IQ motif(s) and a highly divergent tail. MysPDZ also contains the head domain (residues 407–1169) with an ATP binding site (residues 498–505) and an IQ motif (residues 1183–1205) in the neck. Alignment of the amino acid sequence of ATP binding site and IQ motif with other myosins is shown in Figs. 3E and 3F, respectively. Although these regions show high homology with other myosins, we could not find any actin binding site conserved among myosins in the head domain. A coiled-coil domain (residues 1242–1938) in the tail is longer than other reported unconventional myosins, and may mediate dimerization. The remaining COOH-terminal sequence (residues 1938–2035) may form a globular structure because of its hydrophobicity.

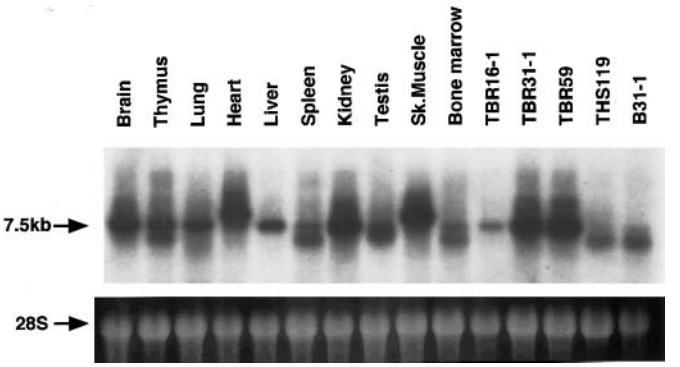

FIG. 4. MysPDZ expression among various tissues and cell lines. THS119 and B31-1 are hematopoietic cell lines. Total RNA were prepared from each tissue and cell line, and 10 μg RNA was applied on each lane. MysPDZ mRNA is observed as 7.5 kb. Different spliced forms were observed in heart, skeletal muscle (Sk. muscle, 10.5 kb), and hematopoietic cells (7.0 kb). 28S indicates the amount of 28S ribosomal RNA.

Expression analysis of MysPDZ mRNA. Northern blot analysis of MysPDZ is shown in Fig. 2. High expression levels of 7.5 kb MysPDZ transcript were detected in highly and intermediate supportive cell lines, but very low levels in poorly supportive cell lines. Next, we analyzed MysPDZ mRNA expression in the various tissues and cell lines. Northern analysis showed that MysPDZ mRNA was detected ubiquitously in all tissues and cell lines, but specific spliced variants were observed in heart, skeletal muscle (10.5 kb) and hematopoietic cells (7.0 kb, Fig. 4).

Expression analysis of MysPDZ protein. To detect MysPDZ protein, we raised anti-MysPDZ antibody us-

FIG. 3. (A) An unrooted phylogenic tree of the myosin superfamily with MysPDZ. The motor domain protein sequences (amino acids 213 to 511 in chicken fast skeletal muscle myosin, GgFsk) of 45 myosins and MysPDZ were aligned with default settings of the ClustalW program and the tree created by TreeView software. MysPDZ does not join any of the existing branches of the tree with greater than 60% confidence. Scale bar indicates 0.1 nucleotide substitutions per site. The accession numbers for the sequences are as follows: class I: Dm IA S45573, Rn Myr4 A53933, Ce IA X75564, Dm IB S45574, Rn Myr2 x74800, Mm IA L00923, Gg Bb U04049, Dd IC L35323, Sc Myo3 P36006, Hs IC U14391, Dd IB P34092, Dd ID P34109, Dd IE Q03479, Dd IA P22467; class II: Sc Myo1 S46773, Eh IIL03534, Dd II P08799, Ac II P05659, Ce IIA P12844, Dm II P05661, Hs Peri P13535, Hs CaA D00943, Ai II A40997, Sm II L01634, Dm nmII Q99323, Hs nmIIA M81105, Gg Sm II P10587; class III: Dm NinaC P10676; class IV: Ac HMWM1 A23622; class V: Mm Dilute X57377, Sc Myo2 P19524; class VI: Dm 95F Q01989, Ss VI A54818; class VII: Hs VIIa U55208; class VIII: At ATM S33812; class IX: Rn Myr5 X77609; class X: Bt X U55042; class XI: At MYA1 Z28389, At MYA2 Z34294; class XII: Ac Myo1 U94397, Ac Myo2 U94398; class XIII: Ce XIII Z266563; class XIV: Tox A Y09693; class XV: Mm myo15 AF053130. (B) Schematic diagram of the domain structure of MysPDZ protein. MysPDZ has a structural organization similar to other myosins consisting of a head domain with ATP binding site (residues 498–505) followed by an IQ motif (residues 1183–1205) in the neck and tail, but no actin binding site is present in the head. Characteristic KE-rich sequence (residues 6–23) and PDZ domain (residues 220–310) exist in the N-terminal. Solid line (residues 1732–1943) indicates the region where the antigen makes antibody against MysPDZ. (C–F) Alignment of the consensus sequence of the KE-rich sequence (C), PDZ domain (D), ATP binding site (E) and IQ motif (F) of MysPDZ with other motif containing molecules. Identical or conserved residues among at least four of the six sequences are shaded. The accession numbers are as follows: (C) Hs MysPDZ AC005412, Mm MAPB P14873, Hs IF-2 O60841, Sc NOP5 Q12499, Sc CBP5 P33322, Dm T2FA, Q05913; (D) Hs MysPDZ AC005412, Hs AF6 P55196, Mm SAP-102 P70175, Rn PSD-95 M96853, Dm DLG1 P31007, Mm ZO1 P39447; (E) Hs MysPDZ D86970, Hs MYH3 P11055, Hs MYH8 P13535, Hs MYH11 P35749, Mm Dilute Q99104; (F) Hs MysPDZ D86970, Hs MYH9 P35579, Hs MYH11 P35749, Hs MYH10 P35580, Hs IQGAP P46940.

FIG. 5. Immunodetection of MysPDZ protein. (A) MysPDZ protein levels positively correlated with the supportive ability of stromal cell lines. TBR52-53 have poorly hematopoietic supportive ability (poorly). TBR59 and TBR311 have highly supportive ability (highly). (B) Anti-MysPDZ antibody detected 230 kDa protein and two additional minor signals. The same band pattern was observed in myc tagged MysPDZ cDNA transfected COS7 cells with anti-myc antibody.

ing rMysPDZ polypeptide [coiled-coil domain (residues 1732–1943), see Fig. 3A] as antigen and examined the expression levels of MysPDZ protein in stromal cell lines. Western blot analysis with anti-MysPDZ antibody detected 230 kDa protein and two additional minor signals (205 and 195 kDa, Fig. 5A). Since the same band pattern was observed in myc tagged MysPDZ cDNA transfected COS-7 cells by anti-myc antibody (Fig. 5B), some of these bands contained degradation products of MysPDZ. As expected, the expression levels of MysPDZ proteins in the stromal cell lines were positively correlated with their hematopoietic supportive ability (Fig. 5A).

Subcellular localization of MysPDZ. To know the subcellular localization of MysPDZ, stromal cells were immunostained with anti-MysPDZ antibody. MysPDZ could be stained even when the cells were permeabilized by 0.5% Triton X-100 before fixation, suggesting that MysPDZ is localized with the cytoskeletal network in the cytoplasm. Under this condition, MysPDZ was present in filamentous and/or network form in the cell (Fig. 6) and this mesh was developed well in a high supportive cell line, TBR311 (Fig. 6A), but poorly in a lower supportive cell line, TBR16-1 (Fig. 6B). In both cell lines, MysPDZ seemed to be slightly concentrated at the perinuclear region. We stained myc tagged MysPDZ-transfected NIH3T3 cells with anti-myc tag antibody, and the exogenous gene products showed similar localization to endogenous MysPDZ (Fig. 6C). As MysPDZ has both myosin-head domain and a KE-rich sequence, which brings association with microtubules, we examined the co-localization of MysPDZ with actin filaments and microtubules in myc tagged MysPDZ transfected NIH3T3 cells. Although partial overlapping was observed, MysPDZ did not totally coincide with either actin filaments or microtubules (Fig. 7).

DISCUSSION

Many studies have reported the importance of direct interaction between hematopoietic cells and stromal cells in hematopoietic organs. Attention has been focused on membrane molecules such as the adhesion molecules, receptors, and their signal transduction pathways. It has recently learned that clustering and

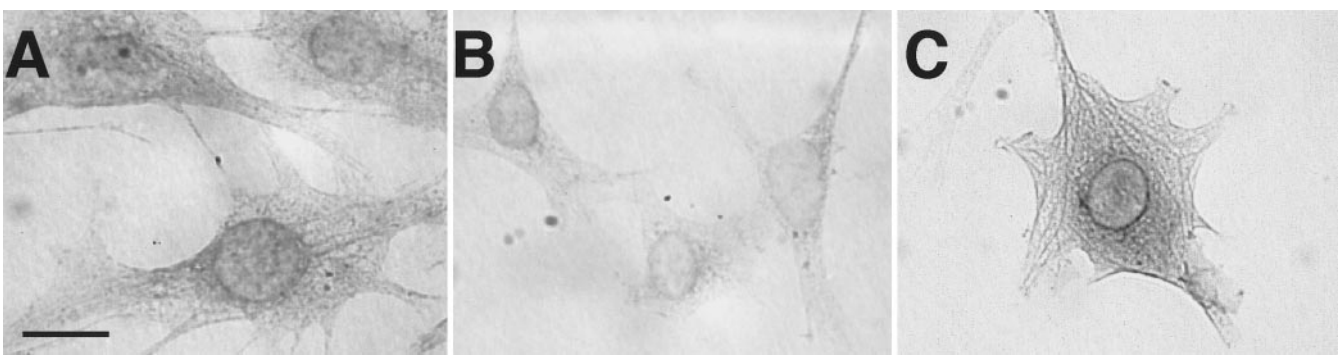

FIG. 6. Immunostaining of MysPDZ in stromal cell lines. Cells were fixed and stained with anti-MysPDZ (A, B) and anti-myc antibody (C). TBR311, a highly supportive cell line, showed filamentous staining for MysPDZ (A), but TBR16-1, a poorly supportive cell line, showed weak staining (B). Myc tagged MysPDZ transfected NIH3T3 cells were stained with anti-myc antibody. The exogenous gene products show localization similar to endogenous MysPDZ (C). Bar indicates 20 μm.

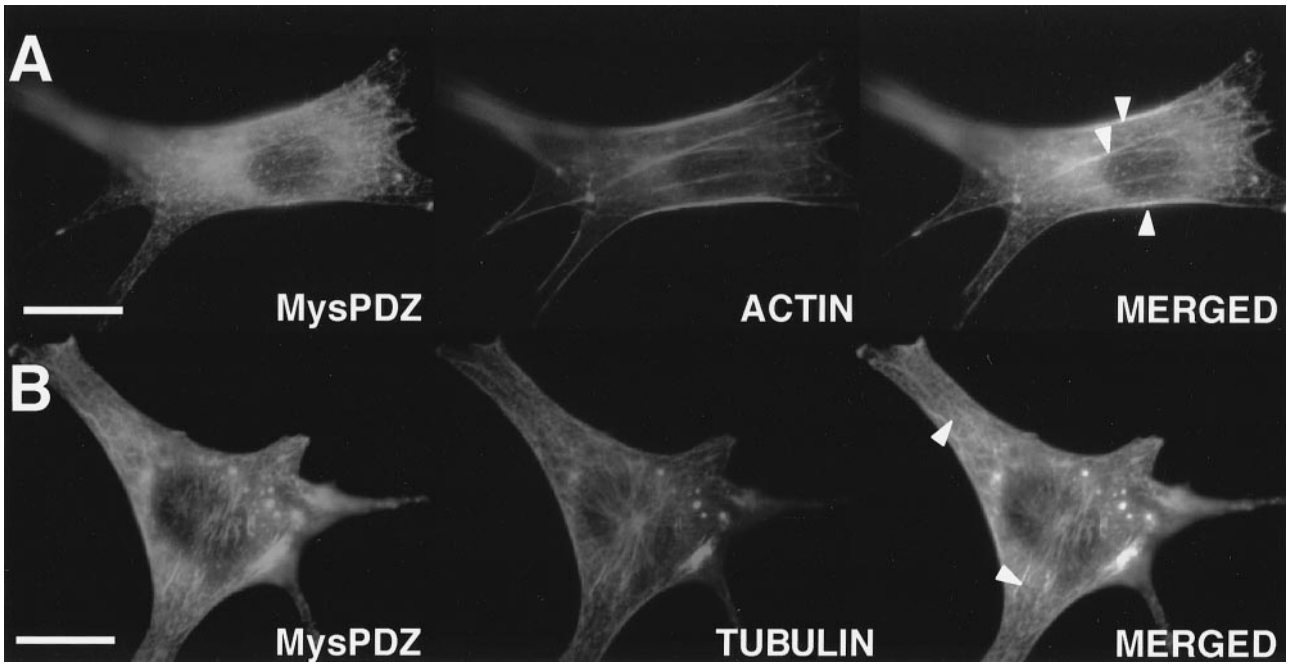

FIG. 7. Fluorescence micrograph of MysPDZ localization in the myc tagged MysPDZ transfected NIH3T3 cells. To double labeling of MysPDZ and actin, MysPDZ was detected by anti-myc antibody followed by FITC-labeled anti-mouse IgG and actin filaments were stained with rhodamine-labeled phalloidin. To double labeling of MysPDZ and microtubules, MysPDZ was detected by anti-MysPDZ antibody followed by FITC-labeled anti-rabbit antibody and microtubules were stained with anti-β-tubulin antibody followed by rhodamine-labeled anti-mouse IgG. MysPDZ localized differentially with actin filaments (A) or microtubules (B), and partial co-localization was observed (merged, arrowheads). Bar indicates 20 μm.

site specific localization of membrane molecules are important for cell to cell communication and these events are regulated by scaffolding proteins such as PDZ containing proteins. Therefore, it is quite intriguing that MysPDZ was isolated as the candidate molecule that may provide the architecture for hematopoietic supportive ability of bone marrow stromal cells. In the nervous system, the PDZ containing proteins, PSD-95/SAP90 (17, 18), DLG (19) and PICK1 (20) are known to regulate the localization and clustering of their target molecules at synaptic contacts. Some PDZ containing proteins such as ZO-1 (21, 22) and affadin (23, 24) function as components of the cell junction in epithelial cells. Multiprotein complexes including PDZ containing proteins are anchored to cytoskeletal filaments like microtubules (25, 26) and actin filaments (27–29), and these events are necessary to enlarge the stability and signal transduction of cell to cell contact. If MysPDZ could anchor its target molecule(s) of the PDZ domain to cytoskeletal proteins without any adaptor molecules, it might be able to act as a direct mediator of signaling between membrane molecules and cytoskeleton at the site of stromal cell-hematopoietic cell contact.

MysPDZ has an ATP binding site and myosin light chains binding IQ motif conserved within myosins, suggesting that this molecule acts as a motor protein regulated by light chains in the presence of ATP. But MysPDZ may not be an actin-based motor protein like other myosins, because it lacks an actin binding site. In fact, it showed different localization with actin filaments in double staining MysPDZ and actin in transfected NIH3T3 cells (Fig. 7A). Since a KE-rich sequence is present in the NH_2-terminal, which allows association with microtubules, we examined but found no co-localization with microtubules (Fig. 7B). MysPDZ thus seems to distribute in filamentous and/or network form independently with these two filaments (Fig. 6). Unconventional myosins generally have short coiled-coil domain and a globular structure at the end of the tail, and therefore do not form a complicated filamentous structure as do class II myosins. MysPDZ has a long coiled-coil domain equal to that of class II myosins, whereas the remaining COOH-terminal sequence consist of 100 amino acids may form a globular structure for its hydrophobicity. We speculate that MysPDZ could not form a filamentous structure by itself and that its subcellular localization may result from the association with other filaments, e.g., class II myosins or intermediate filaments. We are now attempting to confirm the role of the myosin homology region to localize at the cytoskeleton and the effects of a KE-rich sequence and a PDZ domain for its distribution.

Whereas MysPDZ mRNA was detected ubiquitously in all tissues by Northern blot analysis (Fig. 4), alter-

native splicing variants were detected in muscle and hematopoietic cells (Fig. 4). KIAA0216, cloned from a myelogenous leukemia cell line, lacked 458 amino acids at the NH_2-terminal, and we also confirmed that the variants in muscle and hematopoietic cells have a different NH_2-terminal without a KE-rich sequence and a PDZ domain (in preparation). We speculate that the specific variants expressing in muscle and hematopoietic cells may have different roles and distribution.

To date, at least 15 myosin subfamilies have been identified (30) and they have a variety of cellular functions in cell movements (31, 32), membrane trafficking (33–37), organelle particle movement (39, 40), and sensory function (40–43). We propose that MysPDZ is a new member of the myosins because of its divergence from other myosins. Although the biological function of MysPDZ is not clear, it may act as not only a motor protein but also a scaffolding protein involved in cell to cell communication such as stromal cells and hematopoietic cells. Further work is in progress to define the function of MysPDZ including motor activity and target molecule(s) of the PDZ domain.

ACKNOWLEDGMENTS

We thank Kazusa DNA Research Japan for providing KIAA0216 cDNA. This work was supported by a Grant-in-Aid from the Ministry of Education, Science, Sports and Culture of Japan and the Proposal-based New Industry Creative Type Technology R&D Promotion Program from the New Energy and Industrial Technology Development Organization (NEDO) of Japan.

REFERENCES

1. Hunt, P., Robertson, D., Weiss, D., Rennick, D., Lee, F., and Witte, O. N. (1987) *Cell* **48,** 997–1007.
2. Rennick, D., Yang, G., Gemmell, L., and Lee, F. (1987) *Blood* **69,** 682–691.
3. Kittler, E. L., McGrath, H., Temeles, D., Crittenden, R. B., Kister, V. K., and Quesenberry, P. J. (1992) *Blood* **79,** 3168–3178.
4. Koenigsmann, M., Griffin, J. D., DiCarlo, J., and Cannistra, S. A. (1992) *Blood* **79,** 657–665.
5. Zuckerman, K. S., and Wicha, M. S. (1983) *Blood* **61,** 540–547.
6. Campbell, A. D., Long, M. W., and Wicha, M. S. (1987) *Nature* **329,** 744–746.
7. Yanai, N., Sekine, C., Yagita, H., and Obinata, M. (1994) *Blood* **83,** 2844–2850.
8. Dexter, T. M., and Testa, N. G. (1976) *Methods Cell Biol.* **34,** 387–405.
9. Dexter, T. M., Allen, T. D., and Lajtha, L. G. (1977) *J. Cell. Physiol.* **91,** 335–344.
10. Kameoka, J., Yanai, N., and Obinata, M. (1995) *J. Cell. Physiol.* **164,** 55–64.
11. Okuyama, R., Koguma, M., Yanai, N., and Obinata, M. (1995) *Blood* **86,** 2590–2597.
12. Koguma, M., Matsuda, K., Okuyama, R., Yanai, N., and Obinata, M. (1998) *Exp. Hematol.* **26,** 280–287.
13. Nishikawa, S., Sasaki, Y., Kina, T., Amagai, T., and Katsura, Y. (1986) *Immunogenetics* **23,** 137–139.
14. Wu, X., Kocher, B., Wei, Q., and Hammer, J. A., III (1998) *Cell Motil. Cytoskeleton* **40,** 286–303.
15. Lupas, A., Van Dyke, M., and Stock, J. (1991) *Science* **252,** 1162–1164.
16. Nagase, T., Seki, N., Ishikawa, K., Ohira, M., Kawarabayasi, Y., Ohara, O., Tanaka, A., Kotani, H., Miyajima, N., and Nomura, N. (1996) *DNA Res.* **3,** 321–329.
17. Kornau, H. C., Schenker, L. T., Kennedy, M. B., and Seeburg, P. H. (1995) *Science* **269,** 1737–1740.
18. Kim, E., Cho, K. O., Rothschild, A., and Sheng, M. (1996) *Neuron* **17,** 103–113.
19. Tejedor, F. J., Bokhari, A., Rogero, O., Gorczyca, M., Zhang, J., Kim, E., Sheng, M., and Budnik, V. (1997) *J. Neurosci.* **17,** 152–159.
20. Xia, J., Zhang, X., Staudinger, J., and Huganir, R. L. (1999) *Neuron* **22,** 179–187.
21. Furuse, M., Hirase, T., Itoh, M., Nagafuchi, A., Yonemura, S., and Tsukita, S. (1993) *J. Cell Biol.* **123,** 1777–1788.
22. Morita, K., Furuse, M., Fujimoto, K., and Tsukita, S. (1999) *Proc. Natl. Acad. Sci. USA* **96,** 511–516.
23. Mandai, K., Nakanishi, H., Satoh, A., Obaishi, H., Wada, M., Nishioka, H., Itoh, M., Mizoguchi, A., Aoki, T., Fujimoto, T., Matsuda, Y., Tsukita, S., and Takai, Y. (1997) *J. Cell Biol.* **139,** 517–528.
24. Mandai, K., Nakanishi, H., Satoh, A., Takahashi, K., Satoh, K., Nishioka, H., Mizoguchi, A., and Takai, Y. (1999) *J. Cell Biol.* **144,** 1001–1017.
25. Niethammer, M., Valtschanoff, J. G., Kapoor, T. M., Allison, D. W., Weinberg, T. M., Craig, A. M., and Sheng, M. (1998) *Neuron* **20,** 693–707.
26. Brenman, J. E., Topinka, J. R., Cooper, E. C., McGee, A. W., Rosen, J., Milroy, T., Ralston, H. J., and Bredt, D. S. (1998) *J. Neurosci.* **18,** 8805–8813.
27. Hildebrand, J. D., and Soriano, P. (1999) *Cell* **99,** 485–497.
28. Furuyashiki, T., Fujisawa, K., Fujita, A., Madaule, P., Uchino, S., Mishina, M., Bito, H., and Narumiya, S. (1999) *J. Neurosci.* **19,** 109–118.
29. Zhang, W., Vazquez, L., Apperson, M., and Kennedy, M. B. (1999) *J. Neurosci.* **19,** 96–108.
30. Mermall, V., Post, P. L., and Mooseker, M. S. (1998) *Science* **279,** 527–533.
31. Wessels, D., Titus, M., and Soll, D. R. (1996) *Cell Motil. Cytoskeleton* **33,** 64–79.
32. Titus, M. A., Wessels, D., Spudich, J. A., and Soll, D. (1993) *Mol. Biol. Cell* **4,** 233–246.
33. Novak, K. D., Peterson, M. D., Reedy, M. C., and Titus, M. A. (1995) *J. Cell Biol.* **131,** 1205–1221.
34. Jung, G., Wu, X., and Hammer, J. A., 3rd. (1996) *J. Cell Biol.* **133,** 305–323.
35. Geli, M. I., and Riezman, H. (1996) *Science* **272,** 533–535.
36. Goodson, H. V., Anderson, B. L., Warrick, H. M., Pon, L. A., and Spudich, J. A. (1996) *J. Cell Biol.* **133,** 1277–1291.
37. Allen, L. H., and Aderem, A. (1995) *J. Exp. Med.* **182,** 829–840.
38. Huang, J. D., Brady, S. T., Richards, B. W., Stenolen, D., Resau, J. H., Copeland, N. G., and Jenkins, N. A. (1999) *Nature* **397,** 267–270.
39. Wu, X., Bowers, B., Wei, Q., Kocher, B., and Hammer, J. A., III (1997) *J. Cell Sci.* 847–859.
40. Weil, D., Blanchard, S., Kaplan, J., Guilford, P., Gibson, F., Walsh, J., Mburu, P., Varela, A., Levilliers, J., Weston, M. D., Kelley, P. M., Kimberling, W. J., Wagenaar, M., Levi-Acobas, F.,

Larget-Piet, D., Munnich, A., Brown, S. D. M., and Petit, C. (1995) *Nature* **374,** 60–61.

41. Gibson, F., Walsh, J., Mburu, P., Varela, A., Brown, K. A., Antonio, M., Beisel, K. W., Steel, K. P., and Brown, S. D. (1995) *Nature* **374,** 62–64.
42. Porter, J. A., Minke, B., and Montell, C. (1995) *EMBO J.* **14,** 4450–4459.
43. Avraham, K. B., Hasson, T., Steel, K. P., Kingsley, D. M., Russell, L. B., Mooseker, M. S., Copeland, N. G., and Jenkins, N. A. (1995) *Nat. Genet.* **11,** 369–375.